Oil-Encapsulating PEO−PPO−PEO/PEG Shell Cross-Linked Nanocapsules for Target-Specific Delivery of Paclitaxel

Ki Hyun Bae, Yuhan Lee, and Tae Gwan Park*

Department of Biological Sciences, Korea Advanced Institute of Science and Technology, Daejeon 305-701, South Korea

Received September 20, 2006; Revised Manuscript Received November 20, 2006

PEO−PPO−PEO/PEG shell cross-linked nanocapsules encapsulating an oil phase in their nanoreservoir structure was developed as a target-specific carrier for a water-insoluble drug, paclitaxel. Oil-encapsulating PEO−PPO−PEO/PEG composite nanocapsules were synthesized by dissolving an oil (Lipiodol) and an amine-reactive PEO−PPO−PEO derivative in dichloromethane and subsequently dispersing in an aqueous solution containing amine-functionalized six-arm-branched poly(ethylene glycol) by ultrasonication. The resultant shell cross-linked nanocapsules had a unique core/shell architecture with an average size of 110.7 ± 9.9 nm at 37 °C, as determined by dynamic light scattering and transmission electron microscopy. Paclitaxel could be effectively solubilized in the inner Lipiodol phase surrounded by a cross-linked PEO−PPO−PEO/PEG shell layer. The paclitaxel-loaded nanocapsules were further conjugated with folic acid to achieve folate receptor targeted delivery. Confocal microscopy and flow cytometric analysis revealed that folate-mediated targeting significantly enhanced the cellular uptake and apoptotic effect against folate receptor overexpressing cancer cells. The present study suggested that these novel nanomaterials encapsulating an oil reservoir could be potentially applied for cancer cell targeted delivery of various water-insoluble therapeutic and diagnostic agents.

Introduction

Over the past decades, various nanoparticulate carriers such as polymer−drug conjugates, polymeric micelles, nanoparticles, and liposomes have been explored to deliver anticancer agents specifically to cancerous tissues for enhanced therapeutic efficacy and reduced systemic toxicity.[1−5] Among them, hydrogel nanoparticles (nanogels) have attracted growing interest in diverse biomedical applications, including drug delivery, gene delivery, and molecular imaging.[6−9] Nanogels have been extensively investigated as target-specific delivery vehicles for various bioactive macromolecules and anticancer agents because of their nanoscale size (50−200 nm) and thermodynamic stability favorable for intravenous administration and cellular uptake.[10−12] For example, poly(ethylene glycol) nanogels cross-linked with polyethylenimine were ionically interacted with oligonucleotides to form a compact polyelectrolyte complex for targeted penetration of the gastrointestinal epithelium and blood-brain barrier.[13,14] Acid-degradable nanogels were also produced for intracellular delivery of plasmid DNA and proteins via hydrolysis of the polymer chain in acidic lysosomal compartments.[15,16]

PEO−PPO−PEO triblock copolymers are macromolecular surfactants composed of poly(oxyethylene)-*block*-poly(oxypropylene)-*block*-poly(oxyethylene) (Pluronic or Poloxamer series). Interestingly, they undergo self-assembly into spherical micelles in aqueous solution above a critical micelle temperature by hydrophobic interactions between the PPO middle blocks.[17,18] Taking advantage of the temperature-responsive micellization characteristics, we have recently developed a series of PEO−PPO−PEO nanocapsules that can expand and shrink rapidly in response to temperature change.[19−21] These nanocapsules were produced by shell cross-linking of PEO−PPO−PEO copolymers with heparin, polyethylenimine, or gold nanoparticles at an organic/aqueous interface. Polyethylenimine cross-linked PEO−PPO−PEO nanocapsules exhibited a 40-fold volume transition (ca. 332.5 nm at 20 °C and ca. 95.2 nm at 37 °C) and a reversible swelling/shrinking behavior when the temperature was cycled between 20 °C and 37 °C.

In the present study, a new class of PEO−PPO−PEO nanocapsules encapsulating a Lipiodol oil phase in their nanoreservoir structure is presented. Lipiodol is an iodinated derivative of poppy seed oil and has been exploited as a computed tomography (CT) contrast medium, embolic agent, and vehicle for lipophilic anticancer agents such as styrene maleic acid neocarzinostatin (SMANCS) to treat hepatocellular carcinoma.[22−24] For synthesis of Lipiodol-encapsulating PEO−PPO−PEO/PEG nanocapsules, a mixture of Lipiodol and PEO−PPO−PEO copolymer preactivated with an amine-specific reactive group in dichloromethane was ultrasonically emulsified in an aqueous solution containing amine-functionalized six-arm-branched poly(ethylene glycol). The resultant nanocapsules are expected to effectively solubilize water-insoluble anticancer agents in the inner hydrophobic oil phase stabilized by a covalently cross-linked PEO−PPO−PEO/PEG shell layer. Moreover, the drug-loaded nanocapsules were conjugated with folic acid, which is an active recognition moiety for folate receptors highly expressed in several human tumors including ovarian and breast cancers, to achieve tumor-selective targeting.[25−28] The size, shape, and dispersion stability of the nanocapsules were investigated by dynamic light scattering (DLS) and transmission electron microscopy (TEM). The potential of the folate-conjugated nanocapsules as target-specific carriers for paclitaxel was evaluated by examining cellular uptake and apoptosis-inducing effects on KB cells overexpressing folate receptors on its surface.

* To whom correspondence should be addressed. Tel: +82-42-869-2621; fax: +82-42-869-2610; e-mail: tgpark@kaist.ac.kr.

10.1021/bm0608939 CCC: $37.00
Published on Web 01/13/2007

Experimental Section

Materials. PEO−PPO−PEO triblock copolymer ($(PEO)_{100}(PPO)_{65}(PEO)_{100}$, Pluronic F127, M_w = 12 600) was obtained from BASF Corporation (Parsipanny, NJ). Amine-functionalized six-arm-branched poly(ethylene glycol) (M_w = 20 000) was purchased from Sunbio (Walnut Creek, CA). Lipiodol, an iodized ethyl ester of fatty acids from poppy seed oil with 38% iodine by weight, was purchased from Laboratories Guerbet (Aulnay-sous-Bois, France). Paclitaxel obtained from Wako (Osaka, Japan) was >97% (w/w) pure and was used without further purification. Folic acid, *p*-nitrophenyl chloroformate (*p*-NPC), *N*,*N*′-dicyclohexylcarbodiimide (DCC), *N*-hydroxysuccinimide (NHS), 4′,6-diamidino-2-phenylindole (DAPI), and propidium iodide (PI) were purchased from Sigma Chemical Co. (St. Louis, MO). Cell-counting kit-8 (CCK-8) was obtained from Dojindo laboratories (Kumamoto, Japan). All other chemicals were of analytical grade.

Synthesis of Lipiodol-Encapsulating PEO−PPO−PEO/PEG Nanocapsules. Lipiodol-encapsulating PEO−PPO−PEO/PEG nanocapsules were prepared by using an emulsification/solvent evaporation method with modifications.[19,20] PEO−PPO−PEO copolymer was first preactivated with *p*-NPC at its two terminal hydroxyl groups as previously described.[21] A mixture of the activated PEO−PPO−PEO copolymer (50 mg) and Lipiodol (0, 25, 50, or 100% w/w relative to the polymer) dissolved in dichloromethane (200 μL) was added dropwise to an aqueous solution (2 mL, pH 9) containing 10 mg of amine-functionalized six-arm-branched poly(ethylene glycol). As a control experiment, Lipiodol emulsion was prepared with unmodified PEO−PPO−PEO copolymer at the same concentration. The solution was sonicated for 3 min using a Branson sonifier 450 (20 kHz, output control 3) and then was neutralized by HCl. The oil-in-water emulsion was quickly transferred to a rotary evaporator with a water bath set at 40 °C to remove residual dichloromethane. The resultant solution was dialyzed against deionized water by a Spectra/Por dialysis membrane with an MW cutoff of 50 kDa and was subsequently filtered through a 0.45-μm cellulose filter to remove large aggregates.

Characterization of Lipiodol-Encapsulating PEO−PPO−PEO/PEG Nanocapsules. The hydrodynamic diameters of Lipiodol-encapsulating PEO−PPO−PEO/PEG nanocapsules were evaluated by using a dynamic light scattering instrument (Zeta-Plus, Brookhaven, NY). The measurement was carried out in triplicate at a concentration of 6 mg/mL over the temperature range from 9 °C to 37 °C. The amount of Lipiodol encapsulated inside the nanocapsules was measured by spectrophotometric detection of iodine released from Lipiodol by *m*-chloroperbenzoic acid mediated oxidation as previously reported.[29] ^{1}H NMR spectra were recorded for the nanocapsules suspended in chloroform-*d* and D_2O to confirm the encapsulation of Lipiodol. Size and shape of the nanocapsules were evaluated by scanning electron microscopy (SEM) and transmission electron microscopy (TEM). Thirty microliters of the nanocapsule solution (6 mg/mL) was equilibrated and dried on a freshly prepared carbon tape at 37 °C, and then its image was obtained with a Philips 535M scanning electron microscope. The same amount of the solution was deposited onto a 300-mesh carbon-coated copper grid and then was observed by a Zeiss Omega 912 transmission electron microscope. The average particle size was determined by measuring the diameter of more than 50 particles in the SEM and TEM images.

Paclitaxel Loading into Lipiodol-Encapsulating PEO−PPO−PEO/PEG Nanocapsules. Paclitaxel (0.5 mg) was solubilized in the Lipiodol/PEO−PPO−PEO mixture containing 25% (w/w) Lipiodol for preparation of paclitaxel-loaded nanocapsules. The paclitaxel-loaded nanocapsules were lyophilized to measure the loading amount of paclitaxel. Dried samples were immersed in 5 mL of acetonitrile for 1 h to extract paclitaxel from them and then were diluted with an equal volume of deionized water. After filtration through a 0.2-μm cellulose filter, the amount of paclitaxel in the filtrate was analyzed by isocratic reverse-phase high-performance liquid chromatography (HPLC) (1100 series, Agilent Technologies, Palo Alto, United States) using a Waters Spherisorb ODS2 column (5 μm, 4.6 × 250 mm i.d.). The mobile phase consisting of acetonitrile/water (50/50 v/v) was delivered at a flow rate of 1.0 mL/min. Eluted peaks were monitored at 227 nm. The concentration of paclitaxel as low as 10 μg/mL could be reliably detected by the HPLC method.

Conjugation of Folic Acid. Paclitaxel-loaded nanocapsules were conjugated with folic acid. Folic acid (4.4 mg, 10 μmol) dissolved in anhydrous DMSO was reacted with 6 mg (30 μmol) of DCC and 4 mg (30 μmol) of NHS for 30 min to activate the carboxylic acid groups in folic acid. The activated folic acid solution was added to 25 mL of the nanocapsule solution (6 mg/mL). After 1 day of reaction, the product was filtered through a 0.45-μm cellulose filter and then was dialyzed against deionized water (MW cutoff: 50 kDa) for 1 week in a dark room. The amount of conjugated folic acid was determined by the fluorescamine assay.[28]

Paclitaxel Release and Cytotoxicity Studies. For release experiments, 5 mL of paclitaxel-loaded nanocapsules (6 mg/mL) was placed into a dialysis bag with an MW cutoff of 6 kDa. The bag was immersed in 500 mL of phosphate-buffered saline (PBS) supplemented with 0.05% (w/v) Tween 20 at 37 °C. At a given time point, the amount of paclitaxel released into the medium was determined by HPLC as described above. The cytotoxicity of the drug-loaded nanocapsules was evaluated by examining the inhibition of cancer cell growth. The nanocapsule solution was diluted with PBS solution to give a final concentration of paclitaxel from 0.005 to 5 μg/mL. For comparison, Taxol formulation was prepared according to a reference method.[30] Human nasopharyngeal epidermal carcinoma KB cells (folate receptor overexpressing cell line) were seeded in a 96-well plate at a density of 5×10^3 cells per well and were grown in RPMI medium supplemented with 10% (v/v) fetal bovine serum for 24 h at 37 °C. The culture medium was replaced with folate-deficient RPMI medium containing different paclitaxel formulations and was further incubated for 24 h at 37 °C. The number of viable cells was determined by the CCK-8 cell viability assay.[31]

Evaluation of Cellular Uptake and Apoptosis-Inducing Effect of Paclitaxel-Loaded Nanocapsules. KB cells were plated over a cover slide on a six-well plate at a density of 2×10^5 cells per well and were cultivated for 24 h at 37 °C. The cells were incubated with different paclitaxel formulations (1 μg/mL in paclitaxel) in folate-deficient RPMI medium for 24 h at 37 °C. To visualize intracellular uptake, a hydrophobic Nile Red dye was incorporated into the Lipiodol phase within the nanocapsules by simply adding 0.1 mg of Nile Red into the Lipiodol/PEO−PPO−PEO mixture prior to the preparation of paclitaxel-loaded nanocapsules. The cells were fixed with 4% (w/v) formaldehyde solution in PBS and were stored for 20 min at 4 °C. After washing with PBS, the cover slide was stained with DAPI staining solution (0.7 μg/mL DAPI in PBS) for 30 min. The cells were examined by using an LSM510 confocal laser scanning microscope (Carl Zeiss, Germany) equipped with a 364-nm UV laser and 543-nm HeNe laser. For flow cytometric analysis, the cells treated with the different paclitaxel formulations were harvested, were washed with PBS, and then were fixed by slowly adding 70% (v/v) ethanol while gently vortexing. The fixed cells were stored at 4 °C overnight and were incubated with PI staining solution (0.25 mg/mL PI and 0.1 mg/mL RNase A in PBS) at a concentration of 10^6 cells/mL for 30 min at 37 °C. The PI fluorescence of each nucleus was analyzed by a flow cytometer (FACSCalibur) using a CELLQUEST software (PharMingen).

Results and Discussion

As illustrated schematically in Figure 1, Lipiodol-encapsulating PEO−PPO−PEO/PEG shell cross-linked nanocapsules (LP nanocapsules) were produced by shell cross-linking of *p*-NPC-activated PEO−PPO−PEO copolymers with amine-functionalized six-arm-branched poly(ethylene glycol) at the organic/aqueous interface. After the mixture of the activated PEO−PPO−PEO copolymer and Lipiodol in dichloromethane was

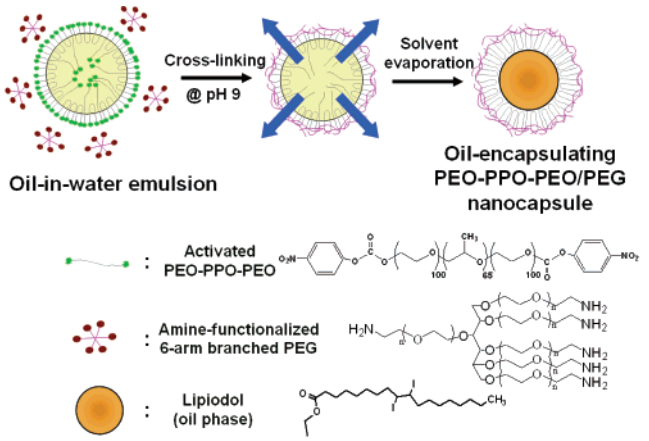

Figure 1. Schematic illustration of the formation of Lipiodol-encapsulating PEO−PPO−PEO/PEG nanocapsules (LP nanocapsules).

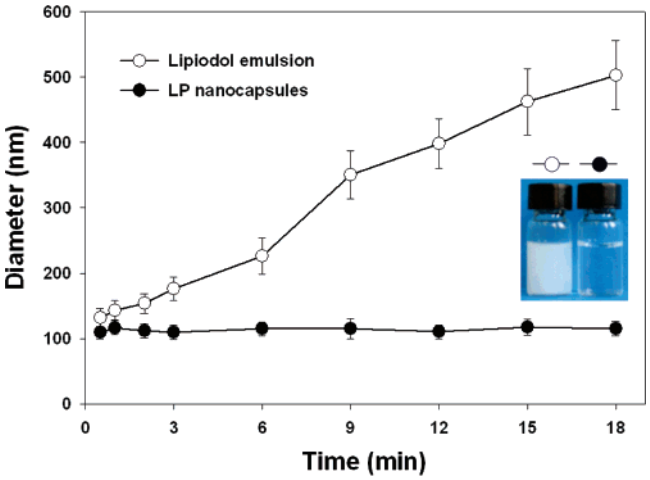

Figure 2. Time course change of hydrodynamic diameter for LP nanocapsules and Lipiodol emulsion. Samples were prepared from 25% (w/w) Lipiodol/PEO−PPO−PEO mixture. The photograph (inset) was taken 15 min after sample preparation.

added into an aqueous solution of amine-functionalized six-arm-branched poly(ethylene glycol), the solution was subjected to ultrasonication to form a stable oil-in-water emulsion.[32,33] The terminal *p*-NPC groups of the PEO−PPO−PEO copolymers were conjugated with primary amine groups in the amine-functionalized six-arm-branched poly(ethylene glycol) at the interface of the oil/water emulsion droplets, resulting in shell cross-linking between the PEO−PPO−PEO and PEG polymers. Once residual solvent within the droplets was evaporated, PEO−PPO−PEO/PEG nanocapsules encapsulating Lipiodol in their nanoreservoir structure were obtained. Since the cross-linking reactions would occur primarily at the organic/aqueous interface, it was conceivable that the resultant nanocapsules had a PEO−PPO−PEO/PEG cross-linked shell structure with an oil-filled core in the interior.

We performed dynamic light scattering (DLS) to examine the dispersion stability of LP nanocapsules compared to the Lipiodol emulsion prepared with unmodified PEO−PPO−PEO copolymer in aqueous solution. As shown in Figure 2, the hydrodynamic diameter of LP nanocapsules was maintained at a range of 110−120 nm at 37 °C, while the mean droplet diameter recorded for the Lipiodol emulsion was drastically increased from 131.9 ± 14.6 nm to 462.2 ± 50.7 nm within 15 min. This droplet growth can be explained by the rapid coalescence of unstable Lipiodol droplets driven by a large interfacial tension difference between the water and Lipiodol

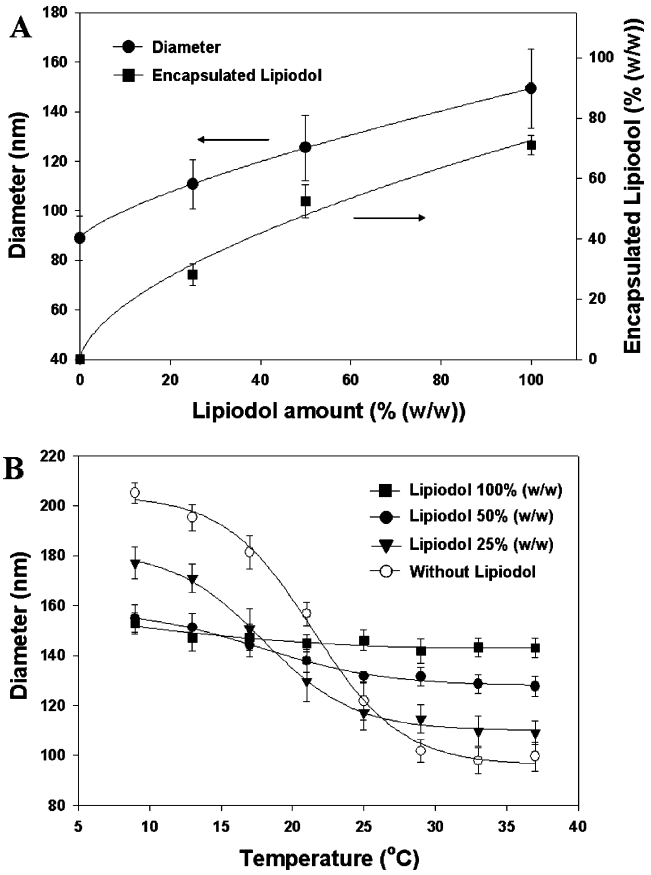

Figure 3. (A) Hydrodynamic diameter of LP nanocapsules and the amount of encapsulated Lipiodol at various weight ratios of Lipiodol/PEO−PPO−PEO. (B) Size change profiles of LP nanocapsules over a temperature range of 9−37 °C.

phases. While the Lipiodol emulsion appeared opaque because of intense scattering of visible light by large oil droplets, LP nanocapsules were transparent. The result suggested that the covalently cross-linked shell layer of the nanocapsules effectively protected the encapsulated oil from coalescence and thus enhanced the stability of the Lipiodol emulsion in aqueous solution.

Figure 3A shows the hydrodynamic diameter of LP nanocapsules and the amount of encapsulated Lipiodol at various weight ratios of Lipiodol/PEO−PPO−PEO. The volume of dichloromethane was kept constant in the formulations. As the weight ratio increased, Lipiodol was encapsulated inside the nanocapsules to a greater extent with a concomitant increase in average diameter of the nanocapsules. The encapsulation efficiency was considerably high; nearly 90% of the Lipiodol was encapsulated at a weight ratio of 25% (w/w). This implies that the volume expansion of nanocapsules loaded with Lipiodol was caused by the fact that Lipiodol was stably encapsulated within the nanocapsules without disturbing the shell structure. Interestingly, the encapsulation of Lipiodol dramatically changed the thermosensitive swelling/shrinking behavior of LP nanocapsules. It has been shown previously that various hollow PEO−PPO−PEO nanocapsules shell cross-linked with heparin, polyethylenimine, or gold nanoparticles exhibited significant volume transitions over a broad temperature range by thermally triggered hydrophobic interactions between the PPO middle blocks of the PEO−PPO−PEO copolymers.[19−21] As shown in Figure 3B, the nanocapsules prepared without Lipiodol greatly changed in diameter from 205.2 ± 4.1 nm to 99.5 ± 5.8 nm upon raising the temperature from 10 °C to 37 °C, which is consistent with the previous findings. However, the volume

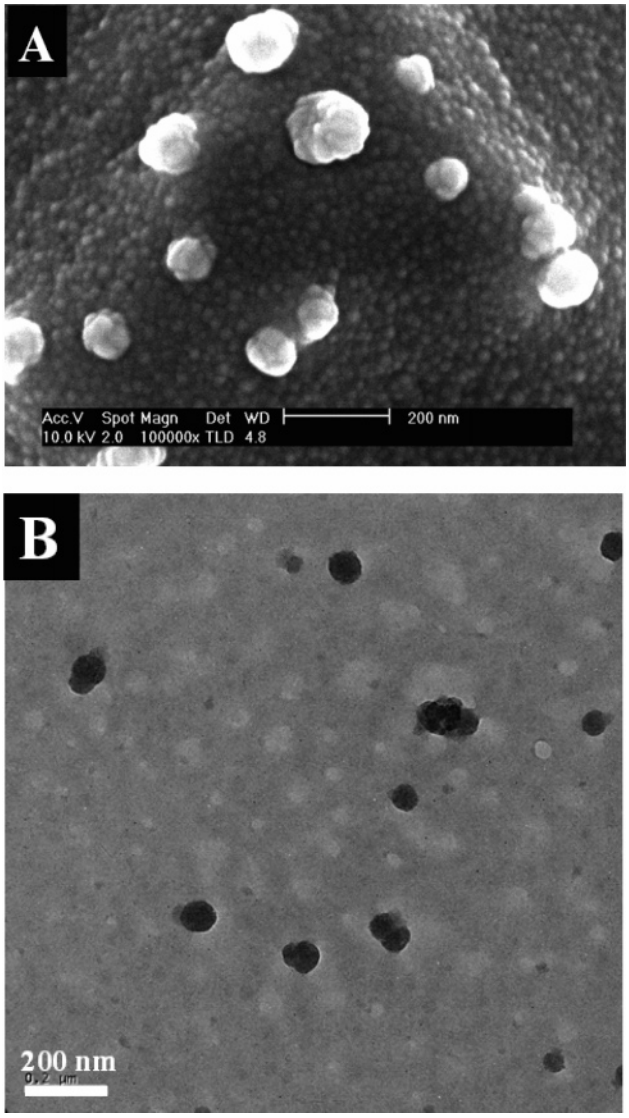

Figure 4. (A) SEM and (B) TEM image of LP nanocapsules prepared from 25% (w/w) Lipiodol/PEO−PPO−PEO mixture. Samples were equilibrated and deposited onto a freshly prepared carbon tape or on a 300-mesh carbon-coated copper grid at 37 °C.

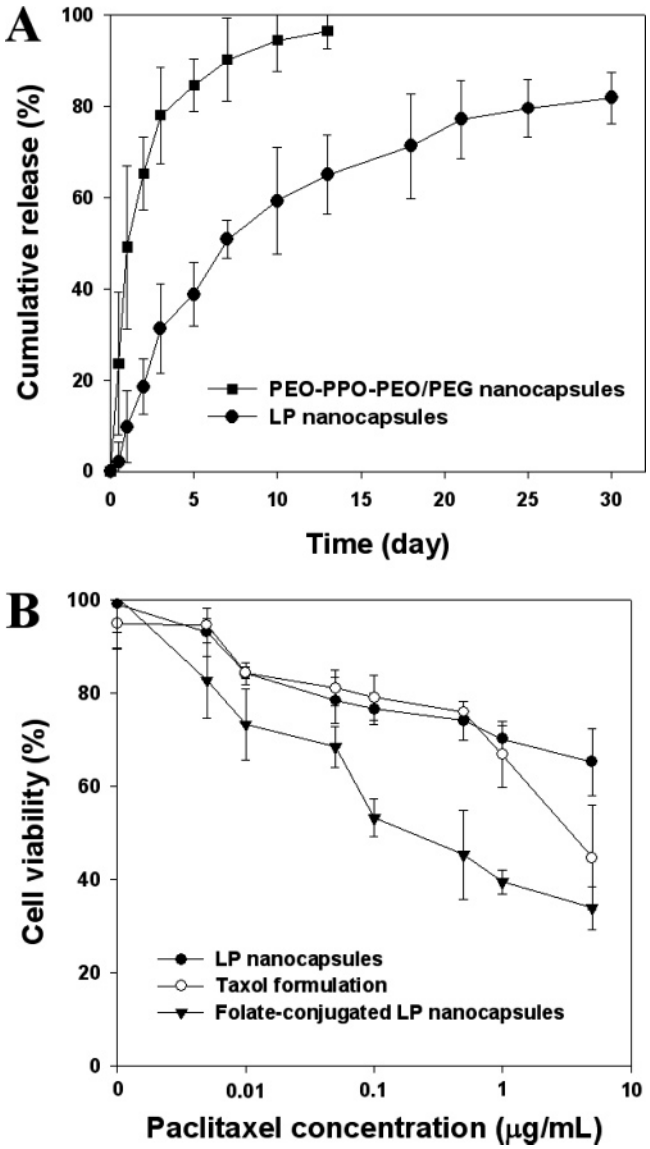

Figure 5. (A) Release profiles of paclitaxel from paclitaxel-loaded LP nanocapsules prepared with or without Lipiodol. (B) Cytotoxicities of different paclitaxel formulations with varying paclitaxel concentrations against KB cells.

transition behavior of LP nanocapsules tended to diminish by increasing the loading amount of Lipiodol. At the same time, the temperature at which they started to swell gradually shifted to a lower temperature. In particular, the nanocapsules prepared at a Lipiodol/PEO−PPO−PEO weight ratio of 100% (w/w) exhibited a marginal degree of volume transition (ca. 152.8 nm at 10 °C and ca. 143.1 nm at 37 °C). This suggests that the shell cross-linked nanocapsules resisted collapsing because of the presence of Lipiodol filled inner cores with increasing temperature, although the cross-linked or grafted PEO−PPO−PEO copolymers tended to self-associate only in the shell layer. Additionally, increased hydrophobic interaction between Lipiodol and PPO segments of the PEO−PPO−PEO copolymers might play an important role in contributing to hamper the temperature-dependent volume transition with increasing Lipiodol content in the nanocapsules.

The morphological characteristics of LP nanocapsules were evaluated by scanning electron microscopy (SEM). Figure 4A presents the SEM image of the nanocapsules taken after preequilibrating at 37 °C. They had a spherical shape with an average diameter of 109.4 ± 25.8 nm. It can be seen that these nanocapsules were well dispersed and separated from each other, indicating that the cross-linked shell framework prevented the encapsulated oil droplets from aggregating into larger ones. It seems that dispersion stability was partly ascribed to the steric stabilization effect of the surface-exposed PEG chains on the nanocapsules.[34−36] We also employed transmission electron

Table 1. Particle Size, Drug Loading Efficiency, and Loading Content of Paclitaxel-Loaded PEO−PPO−PEO/PEG Nanocapsules Prepared with or without Lipiodol

samples ($n = 4$)	particle size (nm)	paclitaxel-loading efficiency (%)	paclitaxel-loading content (wt %)	paclitaxel-loading amount in Lipiodol (mg/mL)
LP nanocapsules	115.8 ± 15.2	46.5 ± 9.5	0.80 ± 0.04	25.8 ± 5.2
PEO−PPO−PEO/PEG nanocapsules	102.7 ± 9.5	12.8 ± 1.9	0.18 ± 0.01	

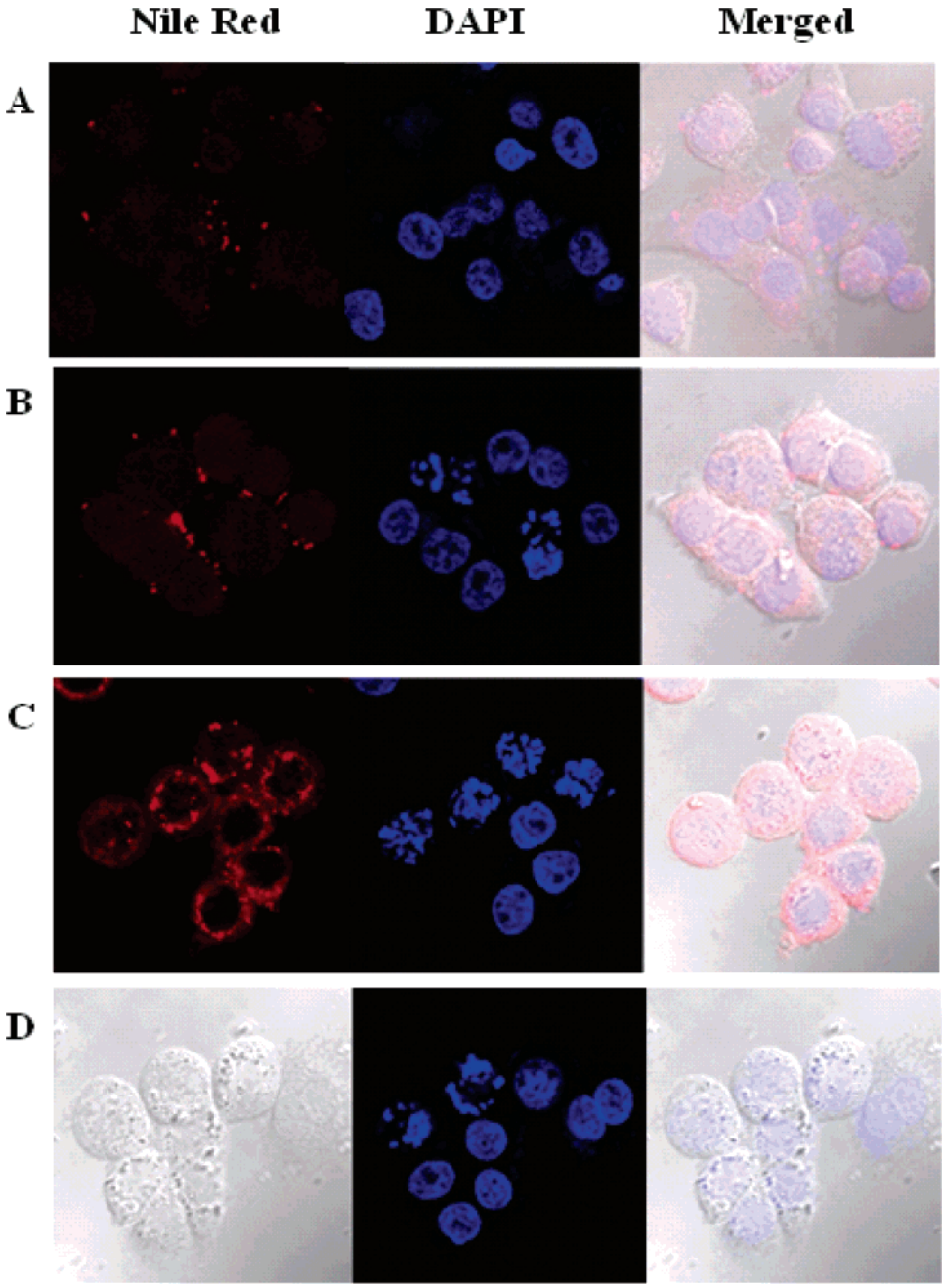

Figure 6. Confocal microscopic images of KB cells following incubation with different paclitaxel formulations at an equivalent drug concentration of 1 μg/mL. LP nanocapsules were fluorescently labeled with Nile Red. Cell nuclei were also stained with DAPI. (A) Control formulation without paclitaxel; (B) LP nanocapsules; (C) folate-conjugated LP nanocapsules; and (D) Taxol formulation.

microscopy (TEM) to examine the interior structure of LP nanocapsules. From the TEM image in Figure 4B, it can be observed that spherical dark spots are well scattered without any significant aggregation. This distinct architecture indicated that the majority of Lipiodol, shown as dark spots because of strong electron scattering, was successfully entrapped in the interior cavities of the nanocapsules. Furthermore, the average size (101.2 $\pm$ 19.4 nm) of the dark contrast regions was consistent with those determined from DLS and SEM results. Therefore, TEM analysis clearly revealed that the nanocapsules had a unique nanoreservoir structure composed of an oil-filled interior with a surrounding polymer shell layer.

As nanosized carriers of Lipiodol, LP nanocapsules are expected to have a good loading capacity of various water-insoluble drugs such as paclitaxel because the hydrophobic core composed of Lipiodol can serve as an ideal microenvironment for the incorporation of lipophilic compounds. To investigate the effect of Lipiodol on drug solubilization, paclitaxel-loaded PEO−PPO−PEO/PEG nanocapsules were prepared with or without Lipiodol. As presented in Table 1, LP nanocapsules exhibited greater solubilization capacity of paclitaxel compared to the formulation without Lipiodol. It was previously reported that hydrophobic compounds could not be sufficiently incorporated in PEO−PPO−PEO copolymer micelles because of the high hydrophilic−lipophilic balance of PEO−PPO−PEO copolymer.[37] The loading amount of paclitaxel in the LP nanocapsules, calculated on the basis of the amount of encapsulated Lipiodol, was slightly higher than the solubility of paclitaxel in Lipiodol solution ($\sim$10 mg/mL), suggesting that the improved solubilization capacity was mainly caused by molecular dissolution of paclitaxel in the inner Lipiodol phase.[23,38] More importantly, the incorporation of paclitaxel did not cause any

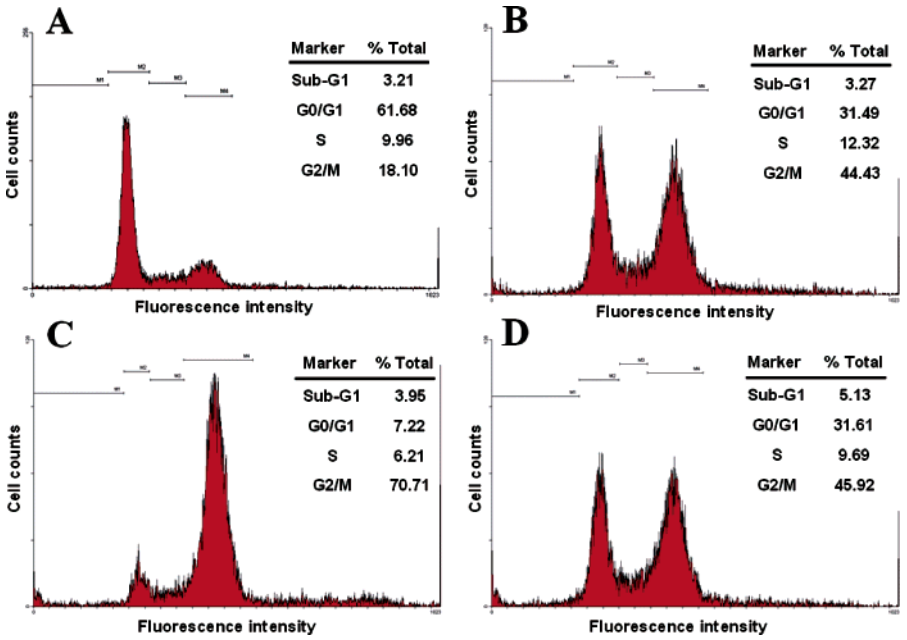

Figure 7. Cell cycle analysis of KB cells after treatment with different paclitaxel formulations at an equivalent drug concentration of 1 μg/mL. (A) Control formulation without paclitaxel; (B) LP nanocapsules; (C) folate-conjugated LP nanocapsules; and (D) Taxol formulation.

significant change in particle size and dispersion stability of the resultant nanocapsules.

Figure 5A presents the release profiles of paclitaxel from the paclitaxel-loaded LP nanocapsules at physiological temperature and pH. LP nanocapsules exhibited a sustained release for 30 days at 37 °C, 80% release in total. However, the release rate from the formulation without Lipiodol was much faster. Approximately 85% of the loaded paclitaxel was released within 5 days with a burst release at the initial stage. The drug release was probably controlled by slow diffusion of paclitaxel as a result of partitioning from the hydrophobic core of the nanocapsules into the aqueous phase. Since paclitaxel was much more solubilized in the oily core than in the aqueous medium, the loaded drug molecules had slowly partitioned out from the nanocapsules as evident from the sustained release behavior. HPLC analysis of the released fractions confirmed that paclitaxel was not chemically changed during the 30-day release period. The 5−6 fold slower release rate of paclitaxel from LP nanocapsules relative to the formulation without Lipiodol suggests the potential applicability of these nanoreservoir materials for intravenous injection. These nanocapsules containing an inner oil phase can be utilized to release various hydrophobic anticancer drugs in a sustained manner in the blood stream. The cytotoxicity of the paclitaxel-loaded nanocapsules was evaluated by measuring the extent of inhibition of cancer cell growth. As shown in Figure 5B, the anticancer effect of paclitaxel-loaded LP nanocapsules was comparable to that of a clinically available formulation of paclitaxel in a 50:50 mixture of Cremophor EL and ethanol (Taxol). The Taxol formulation showed strong cytotoxicity at 5 μg/mL, which was caused mainly by the toxicity of the Cremophor EL vehicle rather than by paclitaxel.[30,39] The folate-conjugated LP nanocapsules exhibited far greater cytotoxicity against KB cells at a lower dosage than the formulations of LP nanocapsules and Taxol. Folate moieties have been shown to significantly improve the intracellular delivery of diverse chemical and biological therapeutic agents via folate receptor-mediated endocytosis.[40−42] Therefore, the result suggested that conjugation of folic acid facilitated cellular uptake of the paclitaxel-loaded LP nanocapsules in a target-specific manner, thereby selectively inhibiting the proliferation of cancer cells.

Cellular uptake and apoptosis-inducing effect of the paclitaxel-loaded LP nanocapsules were investigated in more detail by confocal microscopy and flow cytometric analysis. Figure 6 illustrates the confocal microscopic images of KB cells following incubation with different paclitaxel formulations at an equivalent drug concentration of 1 μg/mL. To visualize subcellular distribution, an inner oil core in the LP nanocapsules was fluorescently labeled with a hydrophobic Nile Red dye. Morphological changes of the cell nuclei were visualized by the DAPI dye staining method to confirm paclitaxel-induced apoptotic cell death.[43] It can be seen that the Nile Red labeled nanocapsules appearing as red fluorescent dots are localized in the cytoplasm, not in the nucleus. The LP nanocapsules without folic acid conjugation were not effectively internalized, suggesting that their cellular uptake was mediated by nonspecific absorptive endocytosis.[39,44] Since the cells treated with the control formulation without paclitaxel were nonapoptotic, strong blue fluorescence was homogeneously detected within the nucleus (Figure 6A). In contrast, after incubation with the paclitaxel-loaded LP nanocapsules or Taxol formulation, the cells displayed apparent evidence of apoptosis such as segregation and fragmentation of cell nucleus into dense and tiny granules (Figure 6B and D). This might be associated with the activation of endogenous nucleases which cleave chromosomal DNA into oligonucleosomal fragments, showing a distinctive ladder pattern in electrophoretic analysis.[45,46] Folate-conjugated and paclitaxel-loaded LP nanocapsules were taken up much more by KB cells than unconjugated LP nanocapsules with greater activity of promoting apoptotic cell death (Figure 6C). Folate receptor-mediated endocytosis might be responsible for the effective cellular uptake and apoptotic effect of the folate-conjugated nanocapsules. The extent of apoptosis was quantitatively assessed by flow cytometric analysis after propidium iodide (PI) staining of the cell nuclei. Since the cytotoxic activity of paclitaxel is attributed to its stabilizing effect on microtubules necessary for spindle formation and cell division, paclitaxel has been shown to cause cell cycle arrest in the G2/M phase and finally cell death through apoptotic mechanisms.[47,48] As shown

in Figure 7, the folate-conjugated LP nanocapsules induced a remarkable accumulation of the G2/M cell population (70.71%), compared to that of the unconjugated LP nanocapsules (44.43%) or Taxol formulation (45.92%). However, the control formulation without paclitaxel showed a similar extent of G2/M phase cells (18.10%) compared to untreated KB cells. Consequently, the above results demonstrated that folate-mediated targeting of paclitaxel-loaded LP nanocapsules significantly enhanced intracellular delivery efficiency and apoptosis-inducing effect.

Conclusions

Our current study demonstrates the potential of Lipiodol-encapsulating PEO−PPO−PEO/PEG nanocapsules as target-specific carriers for paclitaxel. These nanocapsules have a unique nanoreservoir structure composed of an oil-filled interior with a surrounding shell layer. They exhibited greater solubilization capacity of paclitaxel compared to the formulation without Lipiodol because the oil core served as a microenvironment for incorporation of the water-insoluble drug. Moreover, the conjugation of folic acid was shown to facilitate cellular uptake of paclitaxel-loaded nanocapsules via folate receptor-mediated endocytosis, selectively inhibiting proliferation of cancer cells. These novel polymeric nanocapsules with an oil core are expected to be widely used as target-specific delivery vehicles for diverse water-insoluble therapeutic and diagnostic agents.

Acknowledgment. This research was supported by the Ministry of Health and Welfare and the National Research Laboratory program from the Ministry of Science and Technology, Republic of Korea. We thank Soo Hyeon Lee and Gil Woo Chae for apoptosis analysis and Zee-Won Lee in Korea Basic Science Institute (KBSI) for confocal microscopy studies.

References and Notes

(1) Duncan, R. *Nat. Rev. Drug Discovery* **2003**, *2*, 347.
(2) Potineni, A.; Lynn, D. M.; Langer, R.; Amiji, M. M. *J. Controlled Release* **2003**, *86*, 223.
(3) Kataoka, K.; Harada, A.; Nagasaki, Y. *Adv. Drug Delivery Rev.* **2001**, *47*, 113.
(4) Yoo, H. S.; Park, T. G. *J. Controlled Release* **2004**, *96*, 273.
(5) Gabizon, A.; Catane, R.; Uziely, B.; Kaufman, B.; Safra, T.; Cohen, R.; Martin, F.; Huang, A.; Barenholz, Y. *Cancer Res.* **1994**, *54*, 987.
(6) McAllister, K.; Sazani, P.; Adam, M.; Cho, M. J.; Rubinstein, M.; Samulski, R. J.; DeSimone, J. M. *J. Am. Chem. Soc.* **2002**, *124*, 15198.
(7) Nayak, S.; Lee, H.; Chmielewski, J.; Lyon, L. A. *J. Am. Chem. Soc.* **2004**, *126*, 10258.
(8) Missirlis, D.; Tirelli, N.; Hubbell, J. A. *Langmuir* **2005**, *21*, 2605.
(9) Hasegawa, U.; Nomura, S. M.; Kaul, S. C.; Hirano, T.; Akiyoshi, K. *Biochem. Biophys. Res. Commun.* **2005**, *331*, 917.
(10) Maeda, H.; Seymour, L. W.; Miyamoto, Y. *Bioconjugate Chem.* **1992**, *3*, 351.
(11) Jain, R. K. *Adv. Drug Delivery Rev.* **2001**, *46*, 149.
(12) Ferrari, M. *Nat. Rev. Cancer* **2005**, *5*, 161.
(13) Vinogradov, S. V.; Bronich, T. K.; Kabanov, A. V. *Adv. Drug Delivery Rev.* **2002**, *54*, 135.
(14) Vinogradov, S. V.; Batrakova, E. V.; Kabanov, A. V. *Bioconjugate Chem.* **2004**, *15*, 50.
(15) Murthy, N.; Xu, M.; Schuck, S.; Kunisawa, J.; Shastri, N.; Fréchet, J. M. J. *Proc. Natl. Acad. Sci. U.S.A.* **2003**, *100*, 4995.
(16) Goh, S. L.; Murthy, N.; Xu, M.; Fréchet, J. M. J. *Bioconjugate Chem.* **2004**, *15*, 467.
(17) Linse, P.; Malmsten, M. *Macromolecules* **1992**, *25*, 5434.
(18) Mortensen, K.; Pedersen, J. S. *Macromolecules* **1993**, *26*, 805.
(19) Choi, S. H.; Lee, J.-H.; Choi, S.-M.; Park, T. G. *Langmuir* **2006**, *22*, 1758.
(20) Choi, S. H.; Lee, S. H.; Park, T. G. *Biomacromolecules* **2006**, *7*, 1864.
(21) Bae, K. H.; Choi, S. H.; Park, S. Y.; Lee, Y.; Park, T. G. *Langmuir* **2006**, *22*, 6380.
(22) Iwai, K.; Maeda, H.; Konno, T. *Cancer Res.* **1984**, *44*, 2115.
(23) Yoon, C. J.; Chung, J. W.; Park, J. H.; Yoon, Y. H.; Lee, J. W.; Jeong, S. Y.; Chung, H. *Radiology* **2003**, *229*, 126.
(24) Kan, P.; Lin, X.-Z.; Hsieh, M.-F.; Chang, K.-Y. *J. Biomed. Mater. Res. Part B* **2005**, *75*, 185.
(25) Sudimack, J.; Lee, R. J. *Adv. Drug Delivery Rev.* **2000**, *41*, 147.
(26) Allen, T. M. *Nat. Rev. Cancer* **2002**, *2*, 750.
(27) Cho, K. C.; Jeong, J. H.; Chung, H. J.; Joe, C. O.; Kim, S. W.; Park, T. G. *J. Controlled Release* **2005**, *108*, 121.
(28) Oh, I. K.; Mok, H.; Park, T. G. *Bioconjugate Chem.* **2006**, *17*, 721.
(29) Kozutsumi, D.; Ohshiba, Y.; Sugimoto, T.; Tsuboi, H.; Kawashima, A.; Kochiya, M.; Adachi, M.; Takami, M. *Cancer Lett.* **2000**, *158*, 93.
(30) Lee, C. S.; Kim, C.; Kwon, I. C.; Chung, H.; Jeong, S. Y. *J. Controlled Release* **2003**, *89*, 437.
(31) Bae, K. H.; Yoon, J. J.; Park, T. G. *Biotechnol. Prog.* **2006**, *22*, 297.
(32) Varshney, M.; Morey, T. E.; Shah, D. O.; Flint, J. A.; Moudgil, B. M.; Seubert, C. N.; Dennis, D. M. *J. Am. Chem. Soc.* **2004**, *126*, 5108.
(33) Lettow, J. S.; Lancaster, T. M.; Glinka, C. J.; Ying, J. Y. *Langmuir* **2005**, *21*, 5738.
(34) Gref, R.; Minamitake, Y.; Peracchia, M. T.; Trubetskoy, V.; Torchilin, V.; Langer, R. *Science* **1994**, *263*, 1600.
(35) Lee, H.; Jang, I. H.; Ryu, S. H.; Park, T. G. *Pharm. Res.* **2003**, *20*, 818.
(36) Greenwald, R. B.; Choe, Y. H.; McGuire, J.; Conover, C. D. *Adv. Drug Delivery Rev.* **2003**, *55*, 217.
(37) Oh, K. T.; Bronich, T. K.; Kabanov, A. V. *J. Controlled Release* **2004**, *94*, 411.
(38) Lee, I. H.; Park, Y. T.; Roh, K.; Chung, H.; Kwon, I. C.; Jeong, S. Y. *J. Controlled Release* **2005**, *102*, 415.
(39) Soga, O.; van Nostrum, C. F.; Fens, M.; Rijcken, C. J. F.; Schiffelers, R. M.; Storm, G.; Hennink, W. E. *J. Controlled Release* **2005**, *103*, 341.
(40) Lu, Y.; Low, P. S. *Adv. Drug Delivery Rev.* **2002**, *54*, 675.
(41) Yoo, H. S.; Park, T. G. *J. Controlled Release* **2004**, *100*, 247.
(42) Kim, S. H.; Jeong, J. H.; Chun, K. W.; Park, T. G. *Langmuir* **2005**, *21*, 8852.
(43) Tarnowski, B. I.; Spinale, F. G.; Nicholson, J. H. *Biotech. Histochem.* **1991**, *66*, 297.
(44) Savic, R.; Luo, L.; Eisenberg, A.; Maysinger, D. *Science* **2003**, *300*, 615.
(45) Martin, S. J.; Green, D. R.; Cotter, T. G. *Trends Biochem. Sci.* **1994**, *19*, 26.
(46) Bacso, Z.; Everson, R. B.; Eliason, J. F. *Cancer Res.* **2000**, *60*, 4623.
(47) Schiff, P. B.; Horwitz, S. B. *Proc. Natl. Acad. Sci. U.S.A.* **1980**, *77*, 1561.
(48) Jordan, M. A.; Wendell, K.; Gardiner, S.; Derry, W. B.; Copp, H.; Wilson, L. *Cancer Res.* **1996**, *56*, 816.

BM0608939